Hortic. Environ. Biotechnol. 57(1):20-26. 2016.
DOI 10.1007/s13580-016-0019-7

ISSN (print) : 2211-3452
ISSN (online) : 2211-3460

Research Report

Development of a Coupled Photosynthetic Model of Sweet Basil Hydroponically Grown in Plant Factories

Kyoung Sub Park[1,2], Khoshimkhujaev Bekhzod[1], Joon Kook Kwon[1], and Jung Eek Son[2*]

[1]Protected Horticulture Research Institute, National Institute of Horticultural and Herbal Science,
Gyeonsangnam-do 52054, Korea
[2]Department of Plant Science and Research Institute of Agriculture and Life Sciences, Seoul National University,
Seoul 08826, Korea

*Corresponding author: sjeenv@snu.ac.kr

Received October 12, 2015 / Revised November 22, 2015 / Accepted December 25, 2015

Abstract. For the production of plants in controlled environments such as greenhouses and plant factories, crop modeling and simulations are effective tools for configuring the optimal growth environment. The objective of this study was to develop a coupled photosynthetic model of sweet basil (*Ocimum basilicum* L.) reflecting plant factory conditions. Light response curves were generated using photosynthetic models such as negative exponential, rectangular hyperbola, and non-rectangular hyperbola functions. The light saturation and compensation points determined by regression analysis of light curves using modified non-rectangular hyperbola function in sweet basil leaves were 545.3 and 26.5 $\mu mol \cdot m^{-2} \cdot s^{-1}$, respectively. The non-rectangular hyperbola was the most accurate with complicated parameters, whereas the negative exponential was more accurate than the rectangular hyperbola and could more easily acquire the parameters of the light response curves of sweet basil compared to the non-rectangular hyperbola. The CO_2 saturation and compensation points determined by regression analysis of the A-C_i curve were 728.8 and 85.1 $\mu mol \cdot mol^{-1}$, respectively. A coupled biochemical model of photosynthesis was adopted to simultaneously predict the photosynthesis, stomatal conductance, transpiration, and temperature of sweet basil leaves. The photosynthetic parameters, maximum carboxylation rate, potential rate of electron transport, and rate of triose phosphate utilization determined by Sharkey's regression method were 102.6, 117.7, and 7.4 $\mu mol \cdot m^{-2} \cdot s^{-1}$, respectively. Although the A-C_i regression curve of the negative exponential had higher accuracy than the biochemical model, the coupled biochemical model enable to physiologically explain the photosynthesis of sweet basil leaves.

Additional key words: negative exponential, non-rectangular hyperbola, *Ocimum basilicum* L., transpiration

Introduction

The cultivation and consumption of high-quality herbal crops are increasing with improvements in income (Yeo and Lee, 2004). Sweet basil (*Ocimum basilicum* L.) has year-round popularity among consumers (Tesi et al., 1995). Plant factories with artificial lights, in which environmental factors such as light, temperature, humidity, and CO_2 can be controlled, enable stable year-round production, regardless of climate conditions (Son, 1993). Crop modeling and simulation are effective tools for planning plant production due to their usefulness in optimizing the environments in greenhouses and plant factories (Heuvelink, 1999).

Photosynthetic models are fundamental modules in crop growth modeling to include environmental factors such as light, CO_2 concentration, and temperature. Such models are classified into descriptive and biochemical types. The descriptive type of model has the advantage of summarizing the photosynthetic characteristics of crops, while the biochemical type is based on the reaction rate of photosynthetic enzymes and critical limiting rates. A biochemical model called the FvCB model for C3 plants was developed by Farquhar et al. (1980) and has since been widely applied to ecological and physiological research (Medlyn et al, 1999). This model has been improved by inclusion of the rate of triose phosphate utilization (TPU) as an important biochemical limitation (Harley et al., 1992; Sharkey et al., 2007). However, this model is unable to reflect actual crop growth conditions in greenhouses, in which stomatal opening is affected by various environmental factors.

A coupled model of photosynthesis has been developed by combining the FvCB model with stomatal conductance (Leuning, 1995; Nikolov et al., 1995) and energy budget balance (Kim and Lieth, 2003) models. The coupled photosynthetic model considers the biochemical limitations of CO_2 carboxylation as well as the stomatal limitations to the CO_2 supply. Kim and Lieth (2003) developed a coupled model of photosynthesis, stomatal conductance, and transpiration for roses.

Although simple biochemical model for purple basil photosynthesis has been reported by Polyakova (2015), a coupled biochemical model describing actual photosynthetic activity has not been developed. The objective of this study was to develop descriptive and a coupled model of photosynthesis, stomatal conductance, and the transpiration of sweet basil combined with sub-models of stomatal conductance and energy balance.

Materials and Methods

Plant Materials and Cultivation Conditions

Sweet basil (*Ocimum basilicum* L.) seeds were sown on a rock-wool tray (600 mm × 400 mm) on May 12th, 2014 in velno-type greenhouses at the Protected Horticulture Research Institute, Rural Development Administration (RDA) located in Busan, Korea. The seedlings of sweet basil with three to four leaves were transplanted on polystyrene panels (100 mm × 100 mm, φ3 cm) on June 2nd, 2014. The nutrient solution composition for sweet basil was: NO_3^--N 11.6, NH_4^+-N 1.2, P 3.6, K 5.8, Ca 5.8, and Mg 3.0 in meq·L^{-1}, and had an EC of 1.5 dS·m^{-1} (Yeo and Lee, 2004). The hydroponic systems (460 mm × 300 mm × 210 mm) used a deep flow technique at a depth of 70 mm. The nutrient solutions were continuously supplied to the cultivation beds every 10 min at one-hour intervals to maintain the water level in the hydroponic systems. The experiment was conducted in a container-type plant factory (3 m × 12 m). Set-points of room temperature, relative humidity, and CO_2 concentration inside the container-type plant factory were 20°C, 65%, and 400 μmol·mol^{-1}, respectively. The light/dark period was 18 h/6 h and photosynthetic photon flux density (PPFD) was maintained at 150 μmol·m^{-2}·s^{-1} during the light period. Thirty W bar-type LEDs (PGL-PFL600, Parus, Cheonan, Korea) with a 3:7 mixture of blue (445 nm peak) and red (660 nm peak) were used as artificial light sources. The spectral distribution of the light source is shown in Fig. 1.

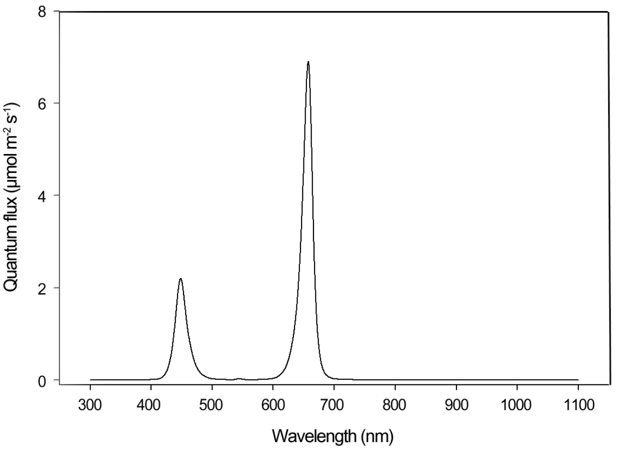

Fig. 1. Spectral distribution of mixed (blue:red = 3:7) light-emitting diode (LED) lights at a distance of 20 cm from the light source in a closed-type plant factory.

Photosynthetic and Optical Properties of Sweet Basil Leaves

The reflectance and transmittance of sweet basil leaves in 300-1,100 nm wavebands at 1 nm intervals were measured using a portable spectro-radiometer with an external integrating sphere (LI-1800, Li-Cor, Lincoln, NE, USA). The reflectance was derived by comparing the wall illumination of the sphere caused by a focused beam of radiation reflected from the leaves. The transmittance was derived by comparing the wall illumination caused by the same radiation that was transmitted through the leaves. The absorbance was calculated as 1 – transmittance – reflectance. The measurements were performed only for the top sides of the leaves.

The net CO_2 assimilation rate and stomatal conductance to water vapor were measured using a portable photosynthesis system (LI-6400, Li-Cor, Lincoln, NE, USA) equipped with an infrared gas analyzer. Fully developed basil leaf was placed across the 6 cm^2 leaf chamber. The temperature of the leaf chamber was maintained at 25°C and relative humidity at 45-65% during the measurements. The net CO_2 assimilation rate as a function of light curves was determined at each step every three to four minutes. Variable PPFDs were beamed from an internal LED light source giving a PPFD range from 0 to 1,500 μmol·m^{-2}·s^{-1} at 400 μmol·mol^{-1} of CO_2 concentration. Regression analyses for descriptive models were conducted for negative exponential (Evans et al., 1993; Eq. 1), rectangular hyperbola (de Wit, 1965; Eq. 2), non-rectangular hyperbola (Thornley, 1976; Eq. 3), and modified non-rectangular (Eq. 4) models, as described below:

$$A = A_{max} * \{(1-\exp(-\alpha * I / A_{max})\} - R_d \qquad \text{(Eq. 1)}$$

$$A = \alpha * A_{max} * I / (\alpha * I + A_{max}) - R_d \qquad \text{(Eq. 2)}$$

$$A = [\alpha * I + A_{max} - \{(\alpha * I + A_{max})^2 - 4\alpha * I * \theta * A_{max}\}^{0.5}] / 2\theta - R_d \qquad \text{(Eq. 3)}$$

$$A = [\alpha * I + A_{max} - \{(\alpha * I + A_{max})^2 - 4\alpha * I * A_{max}\}^{0.5}] / 2\theta - R_d \qquad \text{(Eq. 4)}$$

where A is the net CO_2 assimilation rate ($\mu mol \cdot m^{-2} \cdot s^{-1}$), A_{max} is the maximum net CO_2 assimilation rate ($\mu mol \cdot m^{-2} \cdot s^{-1}$), α parameter is the initial slope, I is the photosynthetic photon flux ($\mu mol \cdot m^{-2} \cdot s^{-1}$), R_d is the respiration rate ($\mu mol \cdot m^{-2} \cdot s^{-1}$), and θ is the curvature of the photosynthetic curve.

The net CO_2 assimilation rate as a function of the A-C_i curve was determined at each step every three to four minutes. Variable CO_2 concentrations were maintained from the photosynthesis measurement system, which resulted in CO_2 concentrations ranging from 100 to 1,500 $\mu mol \cdot mol^{-1}$ at 500 $\mu mol \cdot m^{-2} \cdot s^{-1}$ of PPFD. Sharkey's method (2007) was used to solve the parameters of biochemical models.

A Coupled Biochemical Model of Sweet Basil Photosynthesis

Biochemical models (Eqs. 5-8) were used to acquire the net photosynthetic rate, which has limitations such as the rates of CO_2 carboxylation by Rubisco, Ribulose 1,5-bisphophate (RuBP) regeneration, or triose phosphate utilization:

$$\mathrm{A} = \min\{A_c, A_j, A_p\} - R_d \qquad \text{(Eq. 5)}$$

$$\mathrm{A}_c = V_{max} \frac{C_i - \tau^*}{C_i + K_c * (1 + \frac{O}{K_o})} \qquad \text{(Eq. 6)}$$

$$\mathrm{A}_j = \frac{\mathrm{J} * (C_i - \tau^*)}{4\,(C_i + 2\,\tau^*)} \qquad \text{(Eq. 7)}$$

$$\mathrm{A}_p = 3 * TPU \qquad \text{(Eq. 8)}$$

where A_c is rubisco-imited photosynthetic rate, Aj is RuBP regeneration limited photosynthetic rate through electron transport, Ap is TPU limited photosynthetic rate, V_{max} is the maximum rate of Rubisco carboxylation ($\mu mol \cdot m^{-2} \cdot s^{-1}$), C_i is the intercellular CO_2 concentration ($\mu mol \cdot mol^{-1}$), τ* is the CO_2 compensation point in the absence of R_d ($\mu mol \cdot mol^{-1}$), K_c and K_o are the Michaelis-Menten constants of Rubisco for CO_2 and O_2, respectively ($\mu mol \cdot mol^{-1}$), O is the oxygen partial pressure ($\mu mol \cdot mol^{-1}$), J is the electron transport rate ($\mu mol \cdot m^{-2} \cdot s^{-1}$), and TPU is the triose phosphate utilization rate ($\mu mol \cdot m^{-2} \cdot s^{-1}$).

The intercellular CO_2 concentration in sweet basil leaves was measured by the portable photosynthetic measurement system. Eq. 9 describes the estimating equation Farquhar et al. (1980):

$$\mathrm{c}_i = \frac{\left(g_{tc} - \frac{E}{2}\right) C_a - A}{g_{tc} + E/2} \qquad \text{(Eq. 9)}$$

Where, g_{tc} is total conductance to CO_2 ($\mu mol \cdot mol^{-1}$) and E is transpiration ($mol \cdot m^{-2} \cdot s^{-1}$).

The stomatal conductance was obtained by the Ball, Woodrow and Berry (BWB) model (Ball et al., 1987) and the relative humidity at the leaf surface (h_s) was described as a quadratic function (Eq. 10). The photosynthetic limitation of sweet basil leaves was calculated using an Excel macro program developed by Sharkey et al. (2007):

$$g_s = b + m * A \frac{h_s}{(\frac{C_s}{C_a})} \qquad \text{(Eq. 10)}$$

where g_s ($mol \cdot m^{-2} \cdot s^{-1}$) is the stomatal conductance to water vapor, b ($mol \cdot m^{-2} \cdot s^{-1}$) is the minimum stomatal conductance to water vapor at the light compensation point in the BWB model, m is the empirical coefficient for the sensitivity of g_s, and C_a and C_s are the ambient air and leaf surface CO_2 concentrations ($\mu mol \cdot mol^{-1}$), respectively.

The energy balance model was used to estimate the leaf temperature as a function of g_s, boundary layer conductance, and the environmental parameters such as air temperature, relative humidity, and radiation. The three sub-models of FvCB, BWB, and energy balance were interdependent. The FvCB model used C_i and the leaf temperature (T_L), and included the photosynthetic active radiation value. The BWB model required the net photosynthetic rate (A) and C_i. T_L was estimated iteratively from the energy balance using the air temperature (T_a), conductance for heat, and water vapor. Initially, T_L and C_i were assumed to be equal to T_a and $0.7C_a$, respectively, in order to obtain and estimate A, which was then used to obtain g_s. C_i was estimated using the resulting A and g_s. These processes were solved iteratively using the Newton-Raphson method until C_i and T_L became stable (Kim and Lieth, 2003).

Results and Discussion

Light response curves of sweet basil leaves generated by varying light intensities are shown in Fig. 2. The range at which photosynthetic increases no longer occur due to light increases is the light saturation point. The net CO_2 assimilation rates in the leaves of sweet basil were saturated at about 500 $\mu mol \cdot m^{-2} \cdot s^{-1}$ PPFD, following the initial linear increases with an increasing PPFD up to about 200 $\mu mol \cdot m^{-2} \cdot s^{-1}$ (Fig. 2). The relationship between light intensity and the photosynthetic rate with 100 $\mu mol \cdot m^{-2} \cdot s^{-1}$ PPFD was linear, as reported by Sharp et al. (1984).

Parameters of the negative exponential and rectangular hyperbola models were estimated using regression analysis (Table 1). The negative exponential model ($R^2 = 0.999$) was more accurate for describing the light curve than the rectangular hyperbola model ($R^2 = 0.993$). In addition, the rectangular hyperbola overestimated the photosynthetic value

Table 1. Photosynthetic parameters of the negative exponential (Eq. 1) and rectangular hyperbola (Eq. 2) models calculated from the light response curves of sweet basil in Fig. 2

Parameter	Negative exponential model (R^2 = 0.999)	Rectangular hyperbola model (R^2 = 0.993)
A_{max} (μmol·m^{-2}·s^{-1})[z]	23.9±2.04	31.0±2.92[u]
α (mmol·mol^{-1})[y]	62.1±1.25	79.9±0.86
R_d (μmol·m^{-2}·s^{-1})[x]	2.1±0.07	2.4±0.09
L_{comp} (μmol·m^{-2}·s^{-1})[w]	34.7±0.33	33.0±0.64
L_{sat} (μmol·m^{-2}·s^{-1})[v]	479.0±25.66	493.4±38.71

[z] Maximum photosynthetic capacity
[y] Apparent quantum yield
[x] Dark respiration rate
[w] Light compensation point
[v] Light saturation point
[u] Mean ± standard error (n = 3)

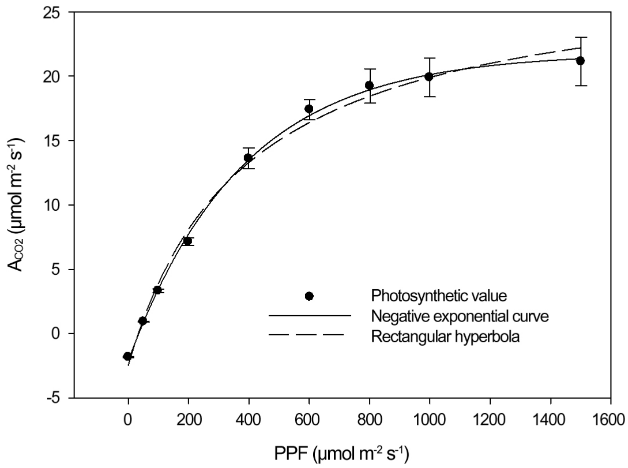

Fig. 2. Regression curves of light response using negative exponential and rectangular hyperbola models at a CO_2 concentration of 400 μmol·mol^{-1} in the leaves of sweet basil. Vertical bars are standard errors of the means from three replications. A_{CO2} and PPF are the CO_2 assimilation rate and the photosynthetic photon flux, respectively.

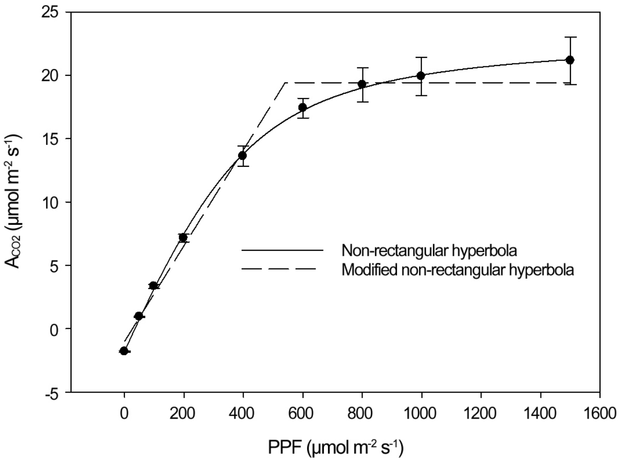

Fig. 3. Regression curves of light response using rectangular hyperbola and non-rectangular hyperbola models at a CO_2 concentration of 400 μmol·mol^{-1} in the leaves of sweet basil. Vertical bars are standard errors of the means from three replications. A_{CO2} and PPF are the CO_2 assimilation rate and the photosynthetic photon flux, respectively.

around the light saturation point more than the negative exponential model (de Wit, 1965; Goudriaan and van Laar, 1978). The initial slope (α) of the non-rectangular hyperbola (Eq. 3) was 52.0 ± 1.92, determined from the measured photosynthetic values ranging from 0 to 100 μmol·m^{-2}·s^{-1} PPFD. The parameters of the negative exponential model were applied to the non-rectangular hyperbola model for curvatures from 200 to 1,500 μmol·m^{-2}·s^{-1} PPFD. The average curvature (θ) of the non-rectangular hyperbola (Eq. 3) for the light curve was 0.8 ± 0.03 by non-linear regression analysis. Thus the low accuracy in the rectangular hyperbola could be compensated for by the non-rectangular hyperbola. Modified non-rectangular hyperbola model has proper method for describing light saturation point using regression analysis without asymptote (Fig. 3 and Table 2)

The residual sum of squares between measured and predicted photosynthetic rates was the lowest at the non-rectangular hyperbola among the three models. The non-rectangular hyperbola showed more accurate predictions under 1,000 μmol·m^{-2}·s^{-1} PPFD and under-estimated predictions over 1,000 μmol·m^{-2}·s^{-1} PPFD compared to the negative exponential model (Fig. 2). The non-rectangular hyperbola and the negative exponential models had higher levels of accuracy than the rectangular hyperbola, and the negative exponential model was enough for describing the light curve.

Regression analysis was applied to the measured photosynthetic rates with increases in CO_2 concentration using the negative exponential model (Fig. 4). The y-axis and x-axis values of the intercept as the estimates of R_d and C_{comp} were 7.9 μmol·m^{-2}·s^{-1} and 85.1 μmol·m^{-2}·s^{-1}. When the intercellular CO_2 concentrations were 62.1 μmol·mol^{-1} at the compensation point and 518.8 μmol·mol^{-1} at the saturation point, their CO_2

Table 2. Photosynthetic parameters of non-rectangular hyperbola (Eq. 3) and modified non-rectangular hyperbola (Eq. 4) models calculated from the light response curves of sweet basil in Fig. 3

Parameter	Non-rectangular hyperbola model (R^2 = 0.999)	Modified non-rectangular hyperbola model (R^2 = 0.993)
A_{max} (μmol·m^{-2}·s^{-1})^z	24.9±2.07^t	28.1±2.56
α (mmol·mol^{-1})^y	52.0±1.92	52.0±1.92
θ^x	0.8±0.03	1.4±0.03
R_d (μmol·m^{-2}·s^{-1})^w	1.8±0.09	1.0±0.18
L_{comp} (μmol·m^{-2}·s^{-1})^v	28.6±2.14	26.5±5.11
L_{sat} (μmol·m^{-2}·s^{-1})^u	419.8±18.69	545.3±48.15

[z] Maximum photosynthetic capacity
[y] Apparent quantum yield
[x] Curvature of curve.
[w] Dark respiration rate.
[v] Light compensation point.
[u] Light saturation point.
[t] Mean ± standard error (n=3).

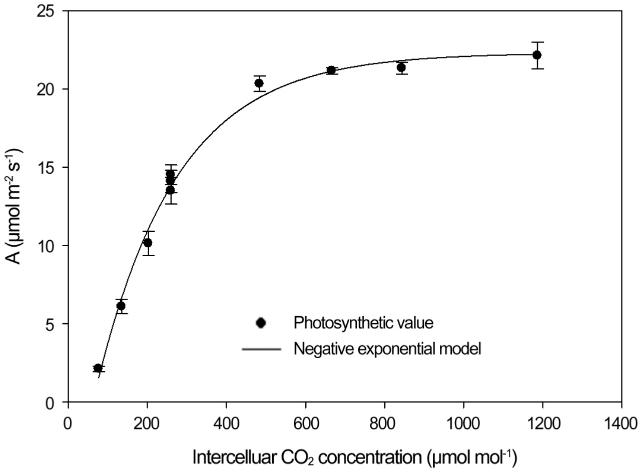

Fig. 4. Net CO_2 assimilation rate (A) as a function of the intercellular CO_2 concentration in the leaves of sweet basil at a photosynthetic photon flux of 500 μmol·m^{-2}·s^{-1}. Vertical bars are the standard errors of the means from the three replications.

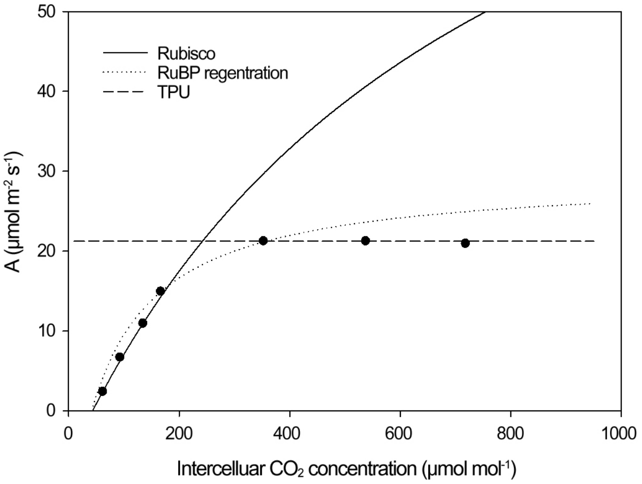

Fig. 5. Predicted net CO_2 assimilation rate (A) as a function of intercellular CO_2 concentration in the leaves of sweet basil at a photosynthetic photon flux of 500 μmol·m^{-2}·s^{-1}. Prediction of photosynthesis assumed Rubisco, RuBP, or TPU limitation.

concentrations (C_{comp} and C_{sat}) of atmosphere were 85.1 and 728.8 μmol·mol^{-1}, respectively (Table 3). The photosynthetic limitation curve (Fig. 5) of sweet basil leaves was obtained using Sharkey's method (2007). As shown in Fig. 5, the predicted intercellular CO_2 concentrations ranged from 100 to 200 μmol·mol^{-1} when determined based on the photosynthetic rate predicted using the Rubisco carboxylation rate, from 200 to 400 μmol·mol^{-1} when determined using the Ribulose 1,5-bisphosphate (RuBP) regeneration rate, and from 400 to 1,000 μmol·mol^{-1} when determined using the triose phosphate utilization rate. It was concluded that the sweet basil photosynthetic A-Ci curve is appropriate to fit the parameters used in Sharkey's method.

The maximum carboxylation rate (V_{max}, μmol·m^{-2}·s^{-1}), the maximum rate of electron transport (J_{max}, μmol·m^{-2}·s^{-1}), the triose phosphate utilization rate (TPU, μmol·m^{-2}·s^{-1}), and the

Table 3. Photosynthetic parameters of the negative exponential model (Eq. 1) calculated from the A-C_i curves of sweet basil in Fig. 3

Parameter	Negative exponential model (R^2 = 0.992)
A_{max} (μmol·m^{-2}·s^{-1})^z	30.3±0.18^u
α (mmol·mol^{-1})^y	148.2±20.76
R_d (μmol·m^{-2}·s^{-1})^x	7.9±0.95
C_{comp} (μmol·mol^{-1})^w	85.1±0.37
C_{sat} (μmol·mol^{-1})^v	728.8±34.58

[z] Maximum photosynthetic capacity.
[y] Apparent quantum yield.
[x] Mitochondrial respiration in the light
[w] CO_2 compensation point.
[v] CO_2 saturation point.
[u] Mean ± standard error (n=3).

Table 4. Estimated photosynthetic parameters of the biochemical model of sweet basil at a leaf temperature of 26.9°C

Parameter	Vmax[z] (µmol·m^{-2}·s^{-1})	Jmax[y] (µmol·m^{-2}·s^{-1})	TPU[x] (µmol·m^{-2}·s^{-1})	R_d[w] (µmol·m^{-2}·s^{-1})	b[v] (mol·m^{-1}·s^{-1})	m[u]
Value	102.6±1.54[t]	117.7±1.16	7.4±0.14	0.7±0.16	0.3172	0.00006

[z] Maximum carboxylation rate
[y] Maximum rate of electron transport
[x] Triose phosphate utilization rate
[w] Mitochondrial respiration in the light
[v] Minimum stomatal conductance to water vapor at the light
[u] Empirical coefficient for the sensitivity of gs to A, Cs, and hs in the BWB model
[t] Mean ± standard error (n =3)

Table 5. Comparison of the residual sum of squares between the measured and predicted photosynthetic rates of the negative exponential and biochemical models of sweet basil

C_i[z] (µmol·mol^{-1})	Measured value (µmol·m^{-2}·s^{-1})	Predicted value (µmol·m^{-2}·s^{-1})	
		Negative exponential model	Biochemical model
77	2.1	1.6	3.7
135	6.1	6.7	9.2
203	10.1	11.1	12.2
260	13.5	13.9	14.0
484	14.5	19.5	16.5
844	21.3	21.8	17.8
Residual sum of squares	-	26.7	33.4

[z] Intercellular CO_2 concentration

mitochondrial respiration in the light (R_d, µmol·m^{-2}·s^{-1}) were 102.6, 117.7, 7.4, and 0.7, respectively (Table 4). These parameters of sweet basil were similar to those of roses calculated by Kim and Lieth (2003), but considerably different from those of purple basil (cv 'Ararat') determined by Polyakakova et al. (2015). These differences might be related differences in cultivars and environmental conditions, such as light sources.

The parameters of minimum stomatal conductance to water vapor at the light compensation point (b) and the empirical coefficient for the sensitivity of g_s, to A, C_s and h_s in the BWB model (m) were solved with linear regression analysis using the measured A-Ci values of sweet basil leaves (Table 4). The parameters of the m value showing the stomatal conductance slope were considerably lower than those of a rose, emphasizing that A-Ci curves should be acquired according to various conditions. The photosynthetic rates could be acquired by inputting their parameters and optical characteristics of sweet basil into the photosynthetic simulator developed by Kim and Lieth (2003).

Overall the residual sum of squares between measured and predicted photosynthetic rates from the coupled biochemical model of photosynthesis, stomata conductance, and transpiration was larger than the residual sum of squares using the negative exponential model (Table 5). The biochemical model underestimated the photosynthetic rate compared to the negative exponential model at a high concentration of CO_2. However, the coupled biochemical model was very effective for physiologically explain sweet basil photosynthesis considering environmental factors and stomatal conductance.

Literature Cited

Ball, J.T., I.E. Woodrow, and J.A. Berry. 1987. A model predicting stomatal conductance and its contribution to the control of photosynthesis under different environmental conditions. Prog. Photosynth. Res. p. 221-224.

de Wit, C.T. 1965. Photosynthesis of leaf canopies. Agricultural Reports 663. Pudoc, Wageningen.

Evans, J.R., I. Jakobsen, and E. Orgren. 1993. Photosynthetic light-response curves 2: Gradients of light absorption and photosynthetic capacity. Planta 189:191-200.

Farquhar, G.D., S. von Caemmerer, and J.A. Berry. 1980. A biochemical model of photosynthetic CO_2 assimilation in leaves of C3 species. Planta 149:78-90.

Goudriaan, J. and H.H. van Laar. 1978. Calculation of daily totals of the gross CO_2 assimilation of leaf canopies. NL. J. Agric. Sci. 26:373-382.

Harley, P.C., R.B. Thomas, J.F. Reynolds, and B.R. Strain. 1992. Modeling photosynthesis of cotton grown in elevated CO_2. Plant Cell Environ. 23:351-363.

Heuvelink, E. 1999. Evaluation of a dynamic simulation model for tomato crop growth a development. Ann. Bot. 83:413-422.

Kim, S.H. and J.H. Lieth. 2003. A coupled model of photosynthesis, stomatal conductance and traspiration for a rose leaf (*Rosa hybrida* L.). Ann. Bot. 91:771-781.

Leuning, R.. 1995. A critical appraisal of a combined stomatal-photosynthesis model. Plant Cell Environ. 18:339-355.

Medlyn, B.E., F.W. Badeck, D.G.G. de Pury, C.V.M. Barton, and M. Broadmeadow. 1999. Effects of elevated CO_2 on photosynthesis in European forest species: a meta-analysis of model parameters. Plant Cell Environ. 22:1475-1495.

Nikolov, N.T., W.J. Massman, and A.W. Shoettle. 1995. Coupling biochemical and biophysical processes at the leaf level: an equilibruium photosynthesis model for leaves of C3 plants. Ecol. Modell. 80:205-235.

Polyakova, M.N., Y.T. Martirosyan, T.A. Dilovaova, and A.A. Kosobryukhov. 2015. Photosynthesis and productivity of Basil Plants (*Ocimum basilicum* L.) under different irradiation. Agric. Biol. 50:124-130.

Sharkey, T.D., C.J. Bernacchi, G.D. Farquhar, and E.L. Sinsaas. 2007. Fitting photosynthetic carbon dioxide response curves for C3 leaves. Plant Cell Environ. 30:1035-1040.

Sharp, R.E., M.A. Mattews, and J.J. Boyer. 1984. Kok effect and the quantum yield of photosynthesis. Plant Physiol. 75:95-101.

Son, J.E. 1993. Plant factory- A prospectiv urban agriculture. J. Bio. Fac. Environ. 2:69-76.

Thornley, J.H.M. 1976. Mathematical models. Plant physiology, Academic Press. London. p. 318.

Tesi, R., G. Chisci, A. Nencini, and R. Tallarico. 1995. Growth response to fertilization of sweet basil (*Ocimum basilicum* L.). Acta Hortic. 390:93-96.

Yeo, K.H. and Y.B. Lee. 2004. The Effect of NO_3^--N and NH_4^+-N ratio in the nutrient solution on growth and quality of sweet basil. Korean J. Hortic. Sci. Technol. 22:37-42.